Nano Energy 52 (2018) 329–335

Contents lists available at ScienceDirect

Nano Energy

journal homepage: www.elsevier.com/locate/nanoen

Full paper

Charge carrier recombination and ion migration in metal-halide perovskite nanoparticle films for efficient light-emitting diodes

Young-Hoon Kim, Christoph Wolf, Hobeom Kim, Tae-Woo Lee*

Department of Materials Science and Engineering, Institute of Engineering Research, Research Institute of Advanced Materials, Nano Systems Institute (NSI), BK21 PLUS SNU Materials Division for Educating Creative Global Leaders, Seoul National University, 1 Gwanak-ro, Gwanak-gu, Seoul 08826, Republic of Korea

ARTICLE INFO

Keywords:
Perovskite nanoparticle film
Light-emitting diodes
Charge carrier confinement
Ion migration
Luminescence efficiency

ABSTRACT

Metal-halide perovskite (MHP) nanoparticles (NPs) have attracted considerable attention as a promising light emitter for efficient light-emitting diodes (LEDs) due to their high color-purity and photoluminescence quantum efficiency (PLQE). In contrast to MHP polycrystalline (PC) bulk films, charge carrier recombination as well as ion migration dynamics in MHP NP films have not been studied yet despite the importance to achieve high electroluminescence efficiency in LEDs. Here, we use steady-state and transient photoluminescence measurements, and photo-responsivity analysis to study the charge carrier recombination and ion migration dynamics in MHP NP films and then, compare these with those of MHP PC films. Results show that MHP NP films do not undergo the severe ion migration and have dominant radiative recombination of excitons by efficiently confining electron-hole pairs. As a result, MHP NP films have high photo-stability, photo-responsibility, and PLQE (> 60%). Our findings provide insight into charge carrier and ion dynamics in MHP NP films, and confirm the potential of NP films for use in efficient LEDs.

1. Introduction

Metal-halide perovskites (MHPs) have attracted considerable attention as a promising light emitter for efficient light-emitting diodes (LEDs) due to narrow emission spectrum (full width at half maximum (FWHM) ~ 20 nm) independent of their grain/particle size, broad emission wavelength tunability, high charge carrier mobility and solution processability [1–8]. Especially, MHP polycrystalline (PC) bulk films have been widely used in LEDs and shown the breakthrough in their device efficiency [2–8]. However, MHP PC films have low photoluminescence quantum efficiency (PLQE) < 40% under low excitation density, possibly due to direct dissociation of excitons into free charge carriers after excitation and inefficient radiative recombination [1,9]. This low PLQE has limited the further growth of luminescence efficiency in LEDs based on MHP PC films [1,9]. Furthermore, under high excitation density, MHP PC films suffer from ion migration, which mainly occurs at grain boundaries in MHP PC films, and Auger non-radiative recombination of charge carriers; these degrade the luminescence efficiency, photo-stability and color purity of emitting light in PC films and LEDs based on PC films [1,9–12].

Colloidal MHP nanoparticles (NPs) are an another form of MHP emitters [1,13–16]. They have spatially confined electron-holr pairs in their small grain/particles (~10 nm) and efficiently passivated surface defects by organic ligands, thus can show efficient radiative recombination of excitons (Fig. 1) [1,13–16]. Low dielectric constant k of organic ligands surrounding NP surfaces (e.g., k of oleic acid ~ 2.5, k of hexylamine ~ 3.8 [17]) and relatively weak van-der-Waals coupling between NPs further confine the electron-hole pairs inside the NPs [9,18]. Surface-passivating organic ligands can also prevent the ion migration in MHP NP films under high excitation density; as a result, MHP NPs can have high PLQE > 70% in solution states [13–15] and PLQE > 60% in film states at both low and high excitation density. For these reasons, they have been intensively applied to demonstrate high efficiency LEDs and have achieved maximum external quantum efficiencies (EQE) up to 13.4% in green emission and EQE up to 6.3% in red emission [19,20]. Therefore, important photophysical characteristics of MHP NPs to achieve high device efficiency in MHP LEDs should be explored.

However, most previous works studied spectroscopic properties of MHP NPs in solution states rather than in film states, so charge carrier recombination dynamics of MHP NP film states are not reported yet. Furthermore, many researchers have analyzed ion migration dynamics in MHP PC films [10,11], but no such work has been performed in MHP NP films. These fundamental properties of MHP NP films should be studied because MHP NP films are directly used in LED applications, and operating stability and luminescence efficiency of NP LEDs are

* Corresponding author.
E-mail addresses: twlees@snu.ac.kr, taewlees@gmail.com (T.-W. Lee).

https://doi.org/10.1016/j.nanoen.2018.07.030
Received 22 May 2018; Received in revised form 6 July 2018; Accepted 13 July 2018
Available online 17 July 2018
2211-2855/ © 2018 Elsevier Ltd. All rights reserved.

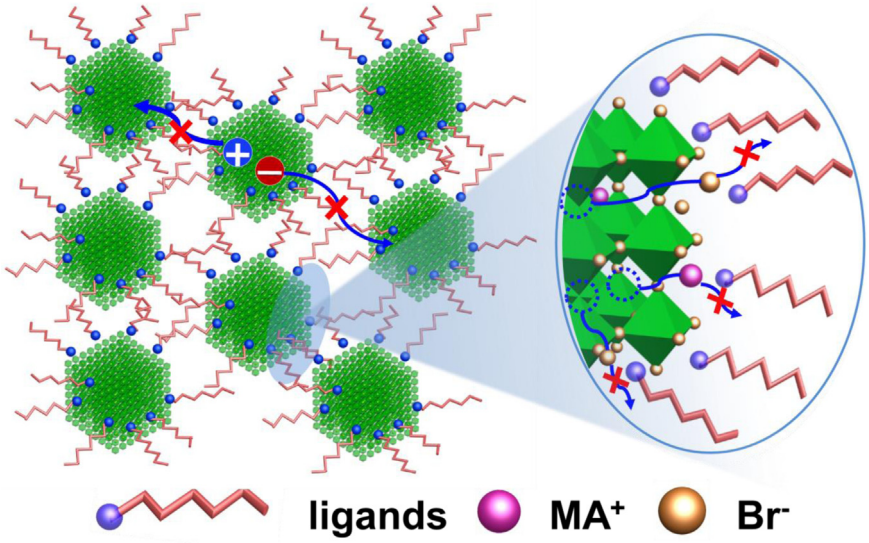

Fig. 1. Schematic illustration of preventing electron-holr pair dissociation and ion migration in MHP NP films.

significantly affected by dynamic behaviors of both charge carrier recombination and ion migration in NP films.

Here, we used steady-state and transient photoluminescence (PL) measurements and photo-responsivity analysis to understand the photo-induced charge carrier recombination and ion migration in MHP NP films, and compare these with those of PC films. MHP NP films (cluster size ~ 50–200 nm due to aggregation or agglomeration during film formation process, PLQE ~ 60.5%) showed exciton recombination as a main mechanism of radiative recombination, on the contrary, MHP PC films with small grains via additive-based nanocrystal pinning process [4] (grain size ~ 50–150 nm, PLQE ~ 36%) had both exciton recombination and bimolecular recombination of free charge carriers for the radiative recombination. Furthermore, surface-passivating organic ligands in MHP NP films efficiently prevented the ion migration and ion-migration-induced defects caused by photo-excitation and thus, showed much reduced defect-related non-radiative recombination and improved photo-stability than did MHP PC films. With these reasons, MHP NP films showed not only higher PLQE (> 60%) but also higher activation energy (E_a ~ 350 meV) of the non-radiative recombination pathways of electron-hole pairs (interpreted as exciton binding energy E_B) [21] at room temperature than did MHP PC films (PLQE < 40% and E_a ~ 98 meV). As a result, we achieved high electroluminescence (EL) efficiency (current efficiency CE ~ 15.5 cd/A)[13] in LEDs (ITO/Buffer hole injection layer (Buf-HIL) [3,13]/MHP NP film /TPBI (1,3,5-tris(N-phenylbenzimia-zole-2-yl)benzene)/LiF/Al). These evidences present that MHP NP films can overcome the limitations of PC films and produce more efficient MHP LEDs.

2. Experimental section

2.1. Synthesis of $MAPbBr_3$ nanoparticles

All synthesis processes of $MAPbBr_3$ NPs were conducted in air at room temperature. To synthesize $MAPbBr_3$ NPs, we dissolved 0.4 mmol of CH_3NH_3Br (Dyesol Ltd.) and 0.4 mmol of $PbBr_2$ (Aldrich, 99.999%) in 10 mL anhydrous DMF (Aldrich, 99.8%) with vigorous stirring for 30 min. Then, we mixed 4 μL of *n*-hexylamine in perovskite solution and 100 μL of oleic acid in 5 mL toluene. After dropping 1 mL perovskite solution into oleic acid-dissolved toluene under mild stirring, the solution immediately changed to bright transparent-green color and then, yellow color within few minutes. Then, the solution was centrifuged at 3000 rpm for 10 min to remove the large aggregated particles. Finally, we attained small $MAPbBr_3$ NPs by collecting the supernatant part in centrifuged solution.

2.2. Fabrication of $MAPbBr_3$ nanoparticle films and bulk films

$MAPbBr_3$ NP films and PC films were formed on top of Buf-HIL. After glasses were cleaned by sonication in acetone and 2-isopropanol for 15 min each and UV-ozone treatment for 10 min, Buf-HIL [3,13] was fabricated by spin-coating and annealing at 150 °C for 30 min. $MAPbBr_3$ NP films were formed by repeating the spin-coating process of $MAPbBr_3$ NP solution and washing process with pure toluene solvent five times to make a layer of 30-nm thickness. $MAPbBr_3$ PC films were fabricated by additive-based nanocrystal pinning method [4]. Both $MAPbBr_3$ NP and PC films were annealed at 90 °C for 10 min to fully evaporate the residual solvent.

2.3. LEDs fabrication

After $MAPbBr_3$ NP films were fabricated on top of ITO patterned glass/Buf-HIL substrate in N_2 glove box, TPBI (50 nm), LiF (1 nm) and Al (100 nm) were thermally deposited sequentially in a high-vacuum (< 10^7 Torr) at rates of 1 Å/s, 0.1 Å/s and 3 Å/s, respectively.

2.4. LEDs characterization

We used Keithley 2400 as a source measurement and Minolta CS2000 as a spectro-radiometer to measure the current-voltage-luminance of LEDs.

2.5. Time-correlated single photon counting (TCSPC) measurement

We used a picosecond-pulse laser head (LDH-P-C-405B, PicoQuant) with 405-nm excitation wavelength as an excitation source and a microchannel plate photo-multiplier tube (MCP-PMT, R3809U-50, Hamamatsu) as a detector. We also used monochromator (SP-2155, Acton) and TCSPC module (PicoHarp, PicoQuant) for spectrally resolving the PL emission and calculating PL lifetimes, respectively.

2.6. Photoluminescence (PL) measurement

PL spectra of MHP NP and PC films were measured using a JASCO FP8500 spectrofluorometer.

2.7. Transmission electron microscopy (TEM) measurement

Transmission electron microscopy (TEM) experiment was performed using a JEOL-JEM 2100 F operating at an acceleration voltage of 200 kV.

3. Results and discussion

MHP NPs were synthesized by using solubility-difference-induced recrystallization method in ambient conditions at room temperature [13,15]. Dimethylformamide (DMF) was used to dissolve the same molar ratio of perovskite precursors (methylammonium bromide (CH_3NH_3Br, MABr), lead bromide ($PbBr_2$)) and *n*-hexylamine, and toluene was used to dissolve the oleic acid and induce the recrystallization of perovskite precursors. When the two solutions were mixed, perovskite precursors were directly recrystallized into MHP NPs because solubility of perovskite precursors rapidly decreased in mixed solutions. Then, pre-dissolved organic ligands adhered to the NPs' surfaces and increased their stability. The solution was centrifuged at 3000 rpm for 10 min, then the supernatant was collected for use in device fabrication. Synthesized MHP NPs were circular dots with diameter ~ 10 nm; the Pb and Br atoms were uniformly distributed inside the NPs and C atoms, which constituted the organic ligands (oleic acid, *n*-hexylamine), were located on the surface of NPs and between NPs (Fig. 2a).

We fabricated MHP NP films on an ITO/buffer-hole injection layer (Buf-HIL) [3,13] substrate by spin-coating process. For comparison, we fabricated MHP PC films on ITO/Buf-HIL by using an additive-based nanocrystal pinning method as previously reported [4]. The resulting perovskite NP films and PC films on Buf-HIL uniformly emitted bright green light under 405-nm excitation (Fig. 2b and Fig. S1, Supporting Information). MHP NP films achieved high *CE* ~ 15.5 cd/A in LEDs (ITO/Buf-HIL/MHP NP film/TPBI/LiF/Al) [13].

We measured excitation laser power-dependent steady-state PL and time-dependent transient PL under the laser excitation to analyze the photo-induced charge carrier recombination and ion migration in MHP NP films and PC films (Fig. 3). The excitation wavelength of laser was fixed at 405 nm and both samples were measured at room temperature under N_2 atmosphere to prevent possible degradation by oxygen. Steady-state PL was measured under the increasing excitation laser power from 0.4 mW to 58 mW (Fig. 3a,b). PL intensity I_{PL} depended on the excitation density L_{EX} as $I_{PL} \sim L_{EX}^{k}$. PL emission mechanism can be elucidated by correlating k value with recombination model of charge carriers as [9,22–25],

$$\frac{dn(t)}{dt} = -k_1 n - k_2 n^2 - k_3 n^3$$

where t is time, n is charge carrier density, k_1 is recombination rate of exciton recombination or trap-related recombination, k_2 is the bimolecular recombination rate of free charge carriers, and k_3 is the Auger (multi charge carrier) recombination rate. In MHP emitters, trap-related recombination and Auger recombination are mostly related to the non-radiative recombination at room temperature, therefore, we can suggest that PL of MHP emitters mostly occurs through exciton recombination or bimolecular recombination of free charge carriers [9,23,26,27]. If PL emission occurs by exciton recombination, the rate of charge carrier recombination in NP films is proportional to the exciton concentration (n) and thus, correlating k value is ~1; otherwise, if PL emission is mainly related to the bimolecular recombination of free charge carriers, the rate of charge carrier recombination is proportional to the free electron concentration multiplied by the free hole concentration (n^2) and therefore I_{PL} has a quadratic dependence on the L_{EX} ($k \sim 2$) [9,23,25].

In our $MAPbBr_3$ PC films, some portion of excitons were directly dissociated into free charge carriers. Therefore, PL occurred through the both recombination mechanisms (i.e. exciton recombination and bimolecular recombination of free charge carriers), and resulted k value ~ 1.36 at $L_{EX} <$ 14 mW (Fig. 3a and Fig. S2a, Supporting Information)

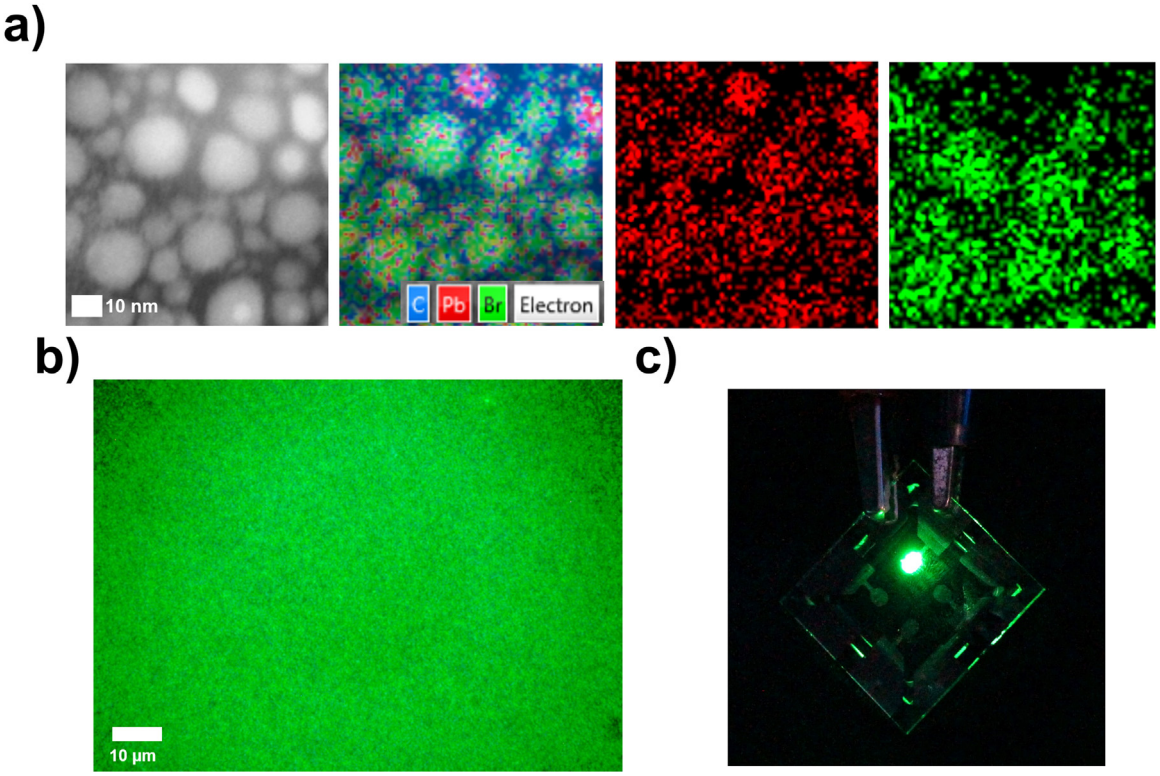

Fig. 2. a) Transmission electron microscopy image and energy dispersive spectroscopy images of MHP NPs, b) fluorescence optical images of NP films and c) operating image of LEDs based on NP films [13].

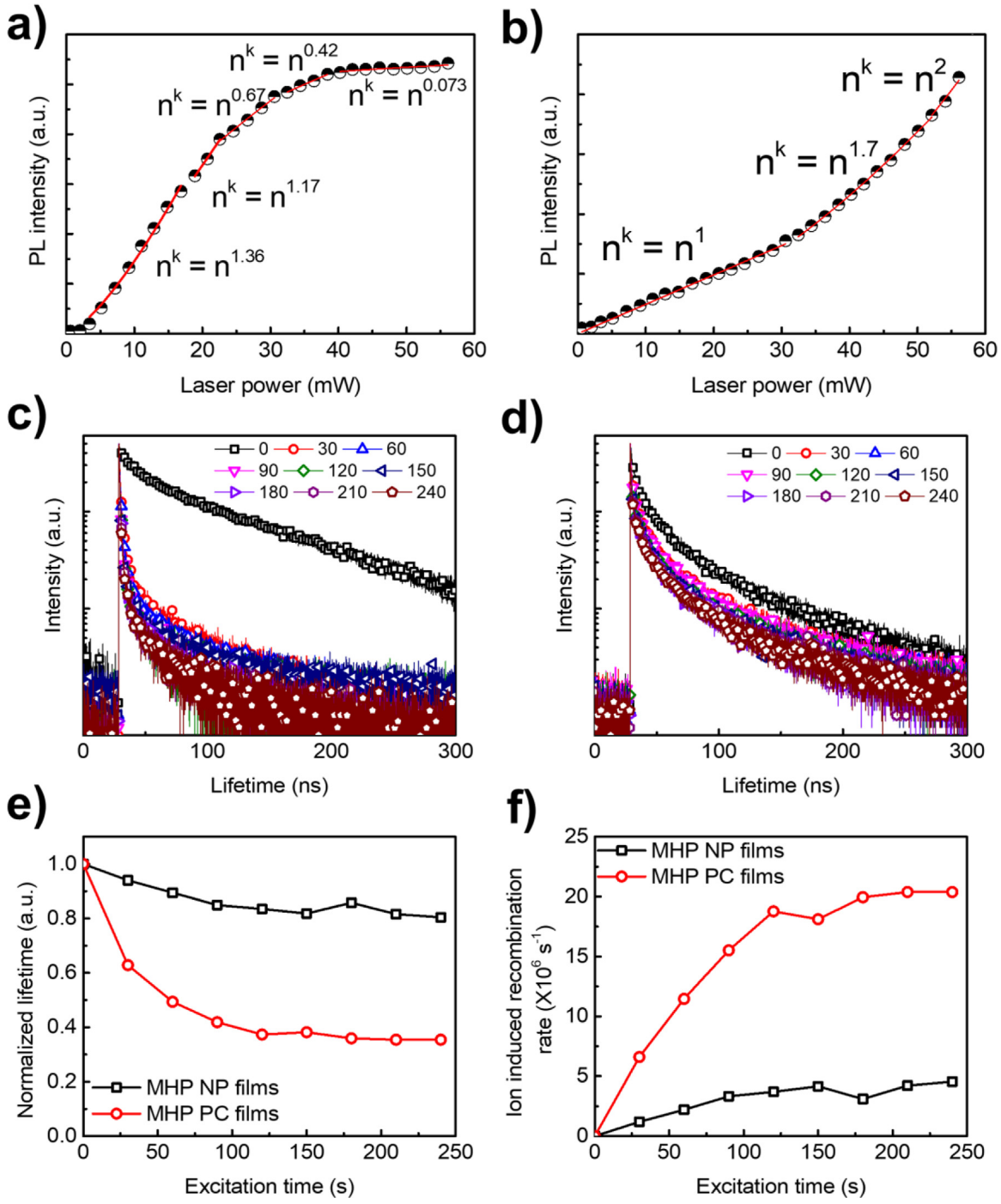

Fig. 3. PL intensities with increasing excitation laser power intensity of a) MHP PC films and b) NP films, and PL lifetimes according to the laser excitation time (s) of c) PC films and d) NP films, e) normalized lifetime and f) ion-induced recombination rate with increasing laser excitation time of PC films and NP films.

[9,23]. As L_{EX} increased, contribution of bimolecular recombination of free charge carriers on PL tended to increase due to scattering and dissociation of excitons into free carriers under the high concentration [9,28,29]; these can be confirmed by the broadening of PL spectrum into higher energy states (into the shorter wavelength) (Fig. S2b, Supporting Information) [24]. The broadening of PL spectrum into lower energy states (into the longer wavelength) is possibly ascribed to the ion-migration-induced defect states under the high laser excitation [26,30]. In spite of increasing ratio of bimolecular recombination of free charge carriers with increasing L_{EX}, the overall k (degree of increase in I_{PL}) of MHP PC films gradually decreased to ~ 0.073 possibly due to 1) luminescence quenching by ion-migration-induced defects under photo-excitation [11], and 2) increasing proportion of non-radiative Auger recombination of multi charge carriers [9,23].

In MHP NP films, I_{PL} was linearly related to L_{EX} (k ~ 1) at L_{EX} < 30 mW (Fig. 3b and Fig. S2c, Supporting Information); this relationship indicates that due to the spatial confinement of electron-hole pairs inside small NPs arising from high E_B (> 100 meV) [15], low k of organic ligands surrounding NP surfaces [17], and weak van-der-Waals coupling between NPs [9,18], PL of NP films is mainly related to the recombination of excitons and thus, rate of charge carrier recombination in NP films is proportional to the exciton concentration (n) [13,15,31,32]. This k value of MHP NP films ~ 1 is in accordance with the result of previous literature (k value of MHP nanocrystal films ~

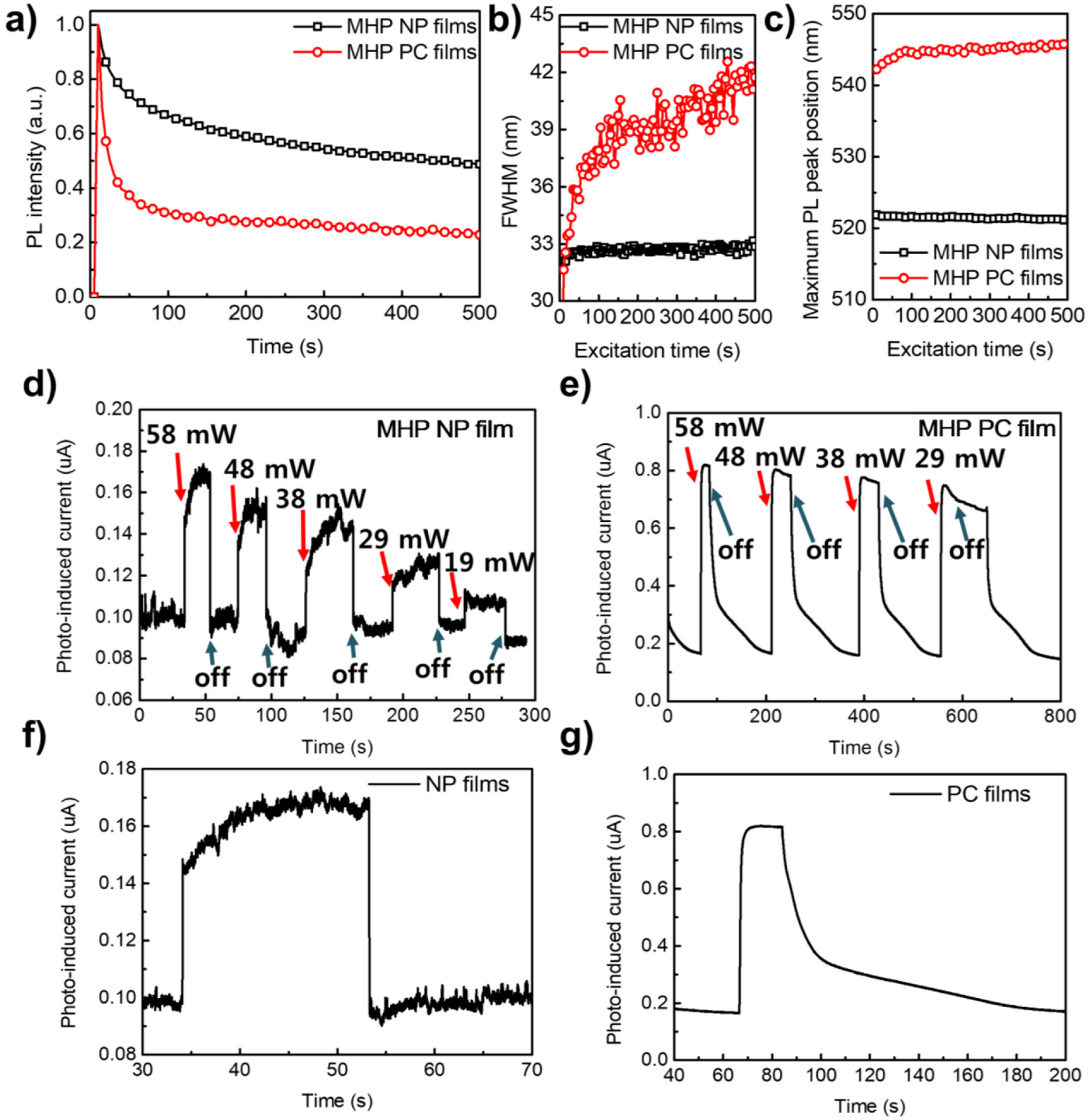

Fig. 4. a) Normalized PL intensities, b) FWHM values and c) maximum PL peak positions of MHP NP films and PC films under constant laser excitation, and photo-induced current and magnified data of d), f) LEDs based on NP films and e), g) LEDs based on PC films at − 2 V bias under gradually-decreasing excitation laser intensity.

1.1) which explains that first-order excitonic recombination is the dominant radiative recombination in MHP nanocrystal films [33]. A large difference between k value of our MHP PC films (~ 1.36) and that of MHP bulk films in the literature (~ 2) is possibly due to the small grain size of 50–150 nm (average grain size ~ 87 nm) in our MHP PC films achieved by additive-based nanocrystal pinning method [4,33,34]. As L_{EX} increased, k of MHP NP films steadily increased from ~ 1.7 to ~ 2 which are quite different from k change with L_{EX} of PC films. We attributed this increase in k of MHP NP films to the arise of bimolecular recombination of free charge carriers as a result of increased charge carrier concentration [9,35]; this can be confirmed by gradually blue-shifted PL peak position from 506.5 nm to 504.5 nm and decreased shoulder peak at lower energy states (at longer wavelength) as L_{EX} increased from 7.16 mW to 58.1 mW (Fig. S2d, Supporting Information). Organic ligands in MHP NP films, which prevent the luminescence quenching caused by ion-migration-induced defect states under the photo-excitation, also assist to increase the overall k (degree of increase in I_{PL}) in NP films. Because of these electron-holr pair confinements and blocking of ion-migration-induced defects, MHP NP films showed exciton recombination as a dominant radiative

recombination pathway, $E_a \sim 350$ meV of the PL quenching process (Fig. S3a,b, Supporting Information) [21], and high PLQE (> 60%) [13]. Whereas, PC films showed both exciton recombination and bimolecular recombination of free charge carriers for the radiative recombination, $E_a \sim 98$ meV of the PL quenching pathways (Fig. S3c,d, Supporting Information) and relatively low PLQE < 40%) [4].

To further study the charge carrier recombination dynamics, we measured time-dependent PL lifetime of MHP PC films and NP films every 30 s under continuous high $L_{EX} \sim 58$ mW with 405-nm excitation wavelength by using time-correlated single-photon counting (TCSPC) (Fig. 3c,d). MHP NP films at excitation time $t_{EX} = 0$ s showed initial average PL lifetime $\tau_{avg} \sim 53.38$ ns, which is much shorter than in PC films ($\tau_{avg} \sim 89.475$ ns). This difference in initial τ_{avg} indicates that luminescence of these two systems occurred mainly by different radiative mechanisms: exciton recombination in MHP NP films; both exciton recombination and bimolecular recombination of free charge carriers in PC films [13,15]. Under illumination for $t_{EX} = 240$ s, MHP NP films showed $\tau_{avg} \sim 42.94$ ns (80% of τ_{avg} at $t_{EX} = 0$ s), whereas in MHP PC films, τ_{avg} was severely reduced to ~ 31.69 ns (35% of τ_{avg} at $t_{EX} = 0$ s) (Fig. 3e). In each type of films, τ_{avg} declined slowly during hundreds of seconds under continuous illumination. These slow decreases in τ_{avg} must be related to the non-radiative recombination induced by photo-excited ion migration rather than to photo-excited charge carrier dynamics [11]. Thus, we conclude that photo-excited ion migration caused many defects in PC films and thereby induced dramatic decrease in τ_{avg} after laser excitation.

Assuming ion-migration and concomitant ion-migration-induced defects dominantly affected on the PL lifetime decrease, the effect of ion migration on τ_{avg} can be further analyzed by calculating recombination rate (reciprocal number of τ_{avg}) difference $K_{ion}(t_{EX})$ between recombination rate at time t_{EX} and recombination rate before laser illumination [11],

$$K_{ion}(t_{EX}) = \frac{1}{(\tau_{avg}(t_{EX}))} - \frac{1}{(\tau_{avg}(0))},$$

where $1/(\tau_{avg}(t_{EX}))$ is recombination rate at time t_{EX} and $1/(\tau_{avg}(0))$ is the recombination rate before laser illumination. $K_{ion}(t_{EX})$ was five times higher in MHP PC films than in NP films (Fig. 3f); this result indicates that photo-illumination easily activates and drives the migration of ions in PC films; therefore ions have a stronger effect on the radiative recombination mechanism in PC films than in NP films. Thus, we suggest that τ_{avg} decreases under photo-illumination in MHP NP films less than in PC films because organic ligands on the surfaces of NPs prevent the ion migration and ion-migration-induced defects in NP films.

Effects of ion migration on radiative recombination can also be quantified by comparing the time-dependent PL spectra of MHP PC films and MHP NP films under the same L_{EX}. MHP NP films had much more stable I_{PL} than did PC films under $L_{EX} \sim 58$ mW (Fig. 4a and Fig. S4, Supporting Information); the difference indicates that easily-activated and mobile ions in MHP PC films cause defects in them, and thereby induced non-radiative recombination of photo-generated charge carriers. These ion-migration-induced defects in MHP PC films were located inside the band-gap of MHP PCs, and therefore induced a red-shifted PL peak position, increasing FWHM of PL from ~20 nm to ~42 nm and shoulder peak at ~590 nm, which was related to the bulk defect states in PC films [30], under laser excitation (Fig. 4b,c and Fig. S4a,b, Supporting Information); these results concur with a previous report that FWHM broadening of perovskite materials is attributed to the scattering of ionized impurities [9,30,36–38]. Laser-illumination can also degrade the MHP PC films by inducing meta-stable states [39], structural transformation [40], halide redistribution [41] or ion segregation [42]. However, these effects did not change the PL spectrum [39–41] or induced the blue-shifted PL spectrum [42,43] rather than red-shifted PL spectrum or shoulder PL peak at longer wavelength. Therefore, we speculate that laser excitation induced the ion migration, and consequently resulted in formation of the ion-migration-induced defects and degraded the MHP PC films.

However, in MHP NP films, the surfaces of NPs are capped with organic ligands that can prevent migration of photo-generated ion impurities between NPs and ion migration-induced defects. Therefore, MHP NP films showed invariant FWHM and peak position of PL spectrum under illumination (Fig. 4a-c and Fig. S4c,d, Supporting Information). This consistence suggests that migration of ions and charge carriers are more prohibited due to better confinement in MHP NP films than in PC films, so the luminescence efficiency and photo-stability can be higher in MHP NP films than in PC films.

The photo-generated ion dynamics can be further studied by comparing the photo-responses of MHP NP and PC films. We measured the photo-induced current of the LEDs based on MHP NP films and PC films (ITO/Buf-HIL/MHP NP film or PC film/TPBI/LiF/Al) under 405-nm laser on/off repetition with gradually decreasing L_{EX} from ~58 mW to ~19 mW. We also applied − 2 V bias to the devices to fully extract the photo-generated current during laser on/off repetition. As L_{EX} decreased from 58 mW to 19 mW, LEDs based on MHP NP films showed gradually decreasing photo-induced current I_{photo} from ~0.17 μA to ~0.11 μA (Fig. 4d). MHP LEDs based on PC film also showed gradually reduced I_{photo} from ~0.8 μA to ~0.7 μA as L_{EX} decreased from 58 mW to 29 mW (Fig. 4e). MHP NP films have lower I_{photo} than do PC films because NP films are much thinner (~30 nm) than PC films (~400 nm) and insulating ligands on the surface of nano-grains in NP films prevent charge carrier transport in films. After the laser was turned off, MHP NP films showed direct decay of I_{photo} within ~0.03 s, while PC films showed significantly slower decay of I_{photo} within ~130 s. The decay time scale of I_{photo} in LEDs based on MHP PC films are on the same time scale with light-activated ion migration and accumulation (> 100 s) [11]. Therefore, we conclude that organic ligands effectively prevent the formation of photo-induced ion-migration in MHP NP films which increase the both photo-stability and photo-response speed.

4. Conclusion

In conclusion, we have studied the charge carrier recombination and ion migration induced by photo-excitation by analyzing steady-state and transient PL and photo-responsivity in MHP NP films comparing with those in MHP PC films. In MHP NP films, I_{PL} increased linearly with increasing L_{EX}, and τ_{avg} were relatively short at $t_{EX} = 0$ s; in contrast, in MHP PC films, I_{PL} increased nearly quadratically with L_{EX}, and τ_{avg} at $t_{EX} = 0$ s was long. These results suggest that the main mechanism of radiative recombination in MHP NP films at low L_{EX} (i.e., at LED working conditions) is exciton recombination rather than bimolecular recombination of free charge carriers due to efficient electron-holr pair confinement and high E_B in small NPs, and organic ligands which have low k and reduce van-der-Waals coupling between NPs. We also revealed that MHP NP films showed an increasing slope of I_{PL} vs. L_{EX}, fast photo-response, and stable I_{PL}, spectrum and τ_{avg} under high L_{EX}. These results indicate that organic ligands in MHP NP films efficiently prevent ion migration and ion-migration-induced defects. These efficient confinement of electron-hole pairs and prevention of ion migration in MHP NP films induced high photo-stability, PLQE and EL efficiency of NP films. Our studies provide insights regarding dynamics of charge carrier recombination and ion migration in MHP NP films and also suggest that use of MHP NP films may overcome the limitations of PC films and achieve efficient MHP LEDs.

Acknowledgements

This work was supported by the National Research Foundation of Korea (NRF) grant funded by the Korea government(MSIT) (NRF-2016R1A3B1908431). All data are available in the main text and the supplementary materials.

Appendix A. Supplementary material

Supplementary data associated with this article can be found in the online version at doi:10.1016/j.nanoen.2018.07.030.

References

[1] Y.-.H. Kim, H. Cho, T.-.W. Lee, Proc. Natl. Acad. Sci. U. S. A. (PNAS) 113, 2016, 11694–11702.
[2] Z.-K. Tan, R.S. Moghaddam, M.L. Lai, P. Docampo, R. Higler, F. Deschler, M. Price, A. Sadhanala, L.M. Pazos, D. Credgington, F. Hanusch, T. Bein, H.J. Snaith, R.H. Friend, Nat. Nanotechnol. 9 (2014) 687–692.
[3] Y.-H. Kim, H. Cho, J.H. Heo, T.-S. Kim, N. Myoung, C.-L. Lee, S.H. Im, T.-W. Lee, Adv. Mater. 27 (2015) 1248–1254.
[4] H. Cho, S.-H. Jeong, M.-H. Park, Y.-H. Kim, C. Wolf, C.-L. Lee, J.H. Heo, A. Sadhanala, N. Myoung, S. Yoo, S.H. Im, R.H. Friend, T.-W. Lee, Science 350 (2015) 1222–1225.
[5] J. Byun, H. Cho, C. Wolf, M. Jang, A. Sadhanala, R.H. Friend, H. Yang, T.-W. Lee, Adv. Mater. 28 (2016) 7515–7520.
[6] M. Yuan, L.N. Quan, R. Comin, G. Walters, R. Sabatini, O. Voznyy, S. Hoogland, Y. Zhao, E.M. Beauregard, P. Kanjanaboos, Z. Lu, D.H. Kim, E.H. Sargent, Nat. Nanotechnol. 11 (2016) 872–877.
[7] N. Wang, L. Cheng, R. Ge, S. Zhang, Y. Miao, W. Zou, C. Yi, Y. Sun, Y. Cao, R. Yang, Y. Wei, Q. Guo, Y. Ke, M. Yu, Y. Jin, Y. Liu, Q. Ding, D. Di, L. Yang, G. Xing, H. Tian, C. Jin, F. Gao, R.H. Friend, J. Wang, W. Huang, Nat. Photonics 10 (2016) 699–704.
[8] Z. Xiao, R.A. Kerner, L. Zhao, N.L. Tran, K.M. Lee, T.-W. Koh, G.D. Scholes, B.P. Rand, Nat. Photonics 11 (2017) 108–115.
[9] G. Xing, B. Wu, X. Wu, M. Li, B. Du, Q. Wei, J. Guo, E.K.L. Yeow, T.C. Sum, W. Huang, Nat. Commun. 8 (2017) 14558.
[10] Y. Yuan, J. Huang, Acc. Chem. Res. 49 (2016) 286–293.
[11] S. Chen, X. Wen, R. Sheng, S. Huang, X. Deng, M.A. Green, A. Ho-baillie, ACS Appl. Mater. Interfaces 8 (2016) 5351–5357.
[12] Y. Shao, Y. Fang, T. Li, Q. Wang, Q. Dong, Y. Deng, Y. Yuan, H. Wei, M. Wang, A. Gruverman, J. Shield, J. Huang, Energy Environ. Sci. 9 (2016) 1752–1759.
[13] Y.-H. Kim, C. Wolf, Y.-T. Kim, H. Cho, W. Kwon, S. Do, A. Sadhanala, C.G. Park, S.-W. Rhee, S.H. Im, R.H. Friend, T.-W. Lee, ACS Nano 11 (2017) 6586–6593.
[14] Y.-H. Kim, G.-H. Lee, Y.-T. Kim, C. Wolf, H.J. Yun, W. Kwon, C.G. Park, T.-W. Lee, Nano Energy 38 (2017) 51–58.
[15] F. Zhang, H. Zhong, C. Chen, X. Wu, X. Hu, H. Huang, J. Han, B. Zou, Y. Dong, ACS Nano 9 (2015) 4533–4542.
[16] L. Protesescu, S. Yakunin, M.I. Bodnarchuk, F. Krieg, R. Caputo, C.H. Hendon, R.X. Yang, A. Walsh, M.V. Kovalenko, Nano Lett. 15 (2015) 3692–3696.
[17] J.O. Saeten, J. Sjoblom, B. Gestblom, J. Phys. Chem. 95 (1991) 1449–1453.
[18] S. Kumar, J. Jagielski, N. Kallikounis, Y.-H. Kim, C. Wolf, F. Jenny, T. Tian, C.J. Hofer, Y.-C. Chiu, W.J. Stark, T.-W. Lee, C.-J. Shih, Nano Lett. 17 (2017) 5277–5284.
[19] X.Y. Chin, A. Perumal, A. Bruno, N. Yantara, S.A. Veldhuis, L. Martinez-Sarti, B. Chandran, V. Chirvony, A. S.-Z. Lo, J. So, C. Soci, M. Gratzel, H.J. Bolink, N. Mathews, S.G. Mhaisalkar, Energy. Environ. Sci. 11 (2018) 1770–1778.
[20] X. Zhang, C. Sun, Y. Zhang, H. Wu, C. Ji, Y. Chuai, P. Wang, S. Wen, C. Zhang, W.W. Yu, J. Phys. Chem. Lett. 7 (2016) 4602–4610.
[21] K. Wu, A. Bera, C. Ma, Y. Du, Y. Yang, L. Li, T. Wu, Phys. Chem. Chem. Phys. 16 (2014) 22476–22481.
[22] Y. Yang, M. Yang, Z. Li, R. Crisp, K. Zhu, M.C. Beard, J. Phys. Chem. Lett. 6 (2015) 4688–4692.
[23] M. Saba, M. Cadelano, D. Marongiu, F. Chen, V. Sarritzu, N. Sestu, C. Figus, M. Aresti, R. Piras, A. Geddo Lehmann, C. Cannas, A. Musinu, F. Quochi, A. Mura, G. Bongiovanni, Nat. Commun. 5 (2014) 5049.
[24] H. He, Q. Yu, H. Li, J. Li, J. Si, Y. Jin, N. Wang, J. Wang, J. He, X. Wang, Y. Zhang, Z. Ye, Nat. Commun. 7 (2016) 10896.
[25] J.M. Richter, M. Abdi-Jalebi, A. Sadhanala, M. Tabachnyk, J.P.H. Rivett, L.M. Pazos-Outón, K.C. Gödel, M. Price, F. Deschler, R.H. Friend, Nat. Commun. 7 (2016) 13941.
[26] D.W. de Quilettes, S.M. Vorpahl, S.D. Stranks, H. Nagaoka, G.E. Eperon, M.E. Ziffer, H.J. Snaith, D.S. Ginger, Science 348 (2015) 683–686.
[27] T. Tachikawa, I. Karimata, Y. Kobori, J. Phys. Chem. Lett. 6 (2015) 3195–3201.
[28] S.D. Stranks, V.M. Burlakov, T. Leijtens, J.M. Ball, A. Goriely, H.J. Snaith, Phys. Rev. Appl. 2 (2014) 34007.
[29] F. Deschler, M. Price, S. Pathak, L.E. Klintberg, D.D. Jarausch, R. Higler, S. Hüttner, T. Leijtens, S.D. Stranks, H.J. Snaith, M. Atatüre, R.T. Phillips, R.H. Friend, J. Phys. Chem. Lett. 5 (2014) 1421–1426.
[30] D. Priante, I. Dursun, M.S. Alias, D. Shi, V.A. Melnikov, T.K. Ng, O.F. Mohammed, O.M. Bakr, B.S. Ooi, Appl. Phys. Lett. 106 (2015) 81902.
[31] J.Q. Grim, S. Christodoulou, F. Di Stasio, R. Krahne, R. Cingolani, L. Manna, I. Moreels, Nat. Nanotechnol. 9 (2014) 891–895.
[32] H.D. Sun, T. Makino, Y. Segawa, M. Kawasaki, A. Ohtomo, K. Tamura, H. Koinuma, Appl. Phys. Lett. 78 (2001) 3385–3387.
[33] F. Yan, J. Xing, G. Xing, L. Quan, S.T. Tan, J. Zhao, R. Su, L. Zhang, S. Chen, Y. Zhao, A. Huan, E.H. Sargent, Q. Xiong, H.V. Demir, Nano Lett. 18 (2018) 3157–3164.
[34] M.-H. Park, S.-H. Jeong, H.-K. Seo, C. Wolf, Y.-H. Kim, H. Kim, J. Byun, J.S. Kim, H. Cho, T.-W. Lee, Nano Energy 42 (2017) 157–165.
[35] H.-H. Fang, R. Raissa, M. Abdu-Aguye, S. Adjokatse, G.R. Blake, J. Even, M.A. Loi, Adv. Funct. Mater. 25 (2015) 2378–2385.
[36] A.D. Wright, C. Verdi, R.L. Milot, G.E. Eperon, M.A. Pe´rez-Osorio, H.J. Snaith, F. Giustino, M.B. Johnston, L.M. Herz, Nat. Commun. 7 (2016) 11755.
[37] J. Lee, E.S. Koteles, M.O. Vassell, Phys. Rev. B 33 (1986) 5512–5516.
[38] X. Wu, M.T. Trinh, D. Niesner, H. Zhu, Z. Norman, J.S. Owen, O. Yaffe, B.J. Kudisch, X.-Y. Zhu, J. Am. Chem. Soc. 137 (2015) 2089–2096.
[39] W. Nie, J.-C. Blancon, A.J. Neukirch, K. Appavoo, H. Tsai, M. Chhowalla, M.A. Alam, M.Y. Sfeir, C. Katan, J. Even, S. Tretiak, J.J. Crochet, G. Gupta, A.D. Mohite, Nat. Commun. 7 (2016) 11574.
[40] R. Gottesman, L. Gouda, B.S. Kalanoor, E. Haltzi, S. Tirosh, E. Rosh-Hodesh, Y. Tischler, A. Zaban, C. Quarti, E. Mosconi, F. De Angelis, J. Phys. Chem. Lett. 6 (2015) 2332–2338.
[41] D.W. DeQuilettes, W. Zhang, V.M. Burlakov, D.J. Graham, T. Leijtens, A. Osherov, V. Bulović, H.J. Snaith, D.S. Ginger, S.D. Stranks, Nat. Commun. 7 (2016) 11683.
[42] O. Hentz, Z. Zhao, S. Gradečak, Nano Lett. 16 (2016) 1485–1490.
[43] M.R. Filip, G.E. Eperon, H.J. Snaith, F. Giustino, Nat. Commun. 5 (2014) 5757.

Young-Hoon Kim received his M.S. (2014) in Division of Environmental Science and Engineering and Ph.D. (2016) in Material Science and Engineering from Pohang University of Science and Technology (POSTECH), Korea. He is currently working in Materials Science and Engineering at Seoul National University, Korea as a post-doctoral researcher (2016–2018). His research focuses on solution-processed electronics based on organic and organic-inorganic hybrid materials for flexible displays and solid-state lightings.

Christoph Wolf received his B.S. and M.S. in Engineering Physics from University of Technology Graz, Austria. He received his Ph.D. in the department of Materials Science and Engineering at Pohang University of Science and Technology (POSTECH). His studies focus on spectroscopy and first-principles calculation of novel semiconductor materials for opto-electronic applications.

Hobeom Kim received his Ph.D. (2017) in the Department of Materials Science and Engineering at Pohang University of Science and Technology (POSTECH), Korea. After his postdoc in Seoul National University (SNU) (2017–2018), Korea, he is currently working in Group for Molecular Engineering of Functional Materials (GMF), Ecole polytechnique fédérale de Lausanne (EPFL), Swiss as a post-doctoral researcher (2018-). His research activity has been focused on optoelectronic devices such as solar cells and light-emitting diodes with organic and perovskite materials.

Tae-Woo Lee is an associate professor in Materials Science and Engineering at Seoul National University, Korea. He received his Ph.D in Chemical Engineering from KAIST, Korea in 2002. He joined Bell Laboratories, USA as a postdoctoral researcher and worked in Samsung Advanced Institute of Technology as a member of research staff (2003–2008). He was an associate professor in Materials Science and Engineering at Pohang University of Science and Technology (POSTECH), Korea until Aug, 2016. His research focuses on printed electronics based on organic and organic-inorganic hybrid materials for flexible displays, solid-state lightings, and solar-energy-conversion devices.